

High pressures and the Kondo gap in $\text{Ce}_3\text{Bi}_4\text{Pt}_3$

J. C. Cooley and M. C. Aronson

Department of Physics, The University of Michigan, Ann Arbor, Michigan 48109-1120

P. C. Canfield

Ames Laboratory, Iowa State University, Ames, Iowa 50011

(Received 20 September 1996)

We have measured the electrical resistivity $\rho(T)$ of single crystals of $\text{Ce}_3\text{Bi}_4\text{Pt}_3$ for temperatures from 1.2 to 300 K, and pressures from 1 bar to 145 kbar. The transport is dominated at high temperatures by excitations across a small activation gap Δ , which increases rapidly with pressure. The low-temperature transport involves variable range hopping among extrinsic states in the gap. The spatial extent of the in-gap states reflects coupling to conduction-electron states, and is strongly modified as pressure enhances Δ . Despite the strong pressure dependence of Δ , a direct correspondence between single-ion energetics and the measured gap is maintained, and the role of valence fluctuations is minimal even at the highest pressures. [S0163-1829(97)00412-8]

The rare-earth and actinide intermetallic “heavy-fermion” compounds are a continuing source of novel and diverse ground states, whose properties are determined not only by the energetics of the spin-compensated moments, but also by the consequences of lattice periodicity.¹ The Kondo insulators have attracted special experimental and theoretical interest, prompted by the possibility that a particularly simple explanation can be made for the origin of the small electronic gap which characterizes its ground state.² Namely, the electronic structure of Kondo insulators is thought to derive from the coherent hybridization of a periodic lattice of Kondo ions.^{3,4} Mean-field solutions³ of the Kondo lattice find that this coherence gap is comparable to the single ion Kondo temperature, at least for small Kondo temperatures and weak mixed valence.

$\text{Ce}_3\text{Bi}_4\text{Pt}_3$ is one of the most heavily studied Kondo insulators. Electrical resistivity measurements, supplemented by thermopower measurements, have identified⁵ a small temperature-dependent gap Δ , whose maximum value is approximately 50 K. Inelastic neutron scattering⁶ and infrared reflectivity measurements⁷ find gaps of 100 and 200 K, respectively. Finally, the electronic specific heat⁵ at the lowest temperatures is smaller than the isostructural, weakly interacting metallic analog $\text{La}_3\text{Bi}_4\text{Pt}_3$, indicating a vanishingly small density of states at the Fermi level. Taken together, these measurements argue convincingly that the Fermi level in $\text{Ce}_3\text{Bi}_4\text{Pt}_3$ lies in a small gap, and that the origin of the gap lies with correlations among the conduction electrons. Core-level spectroscopy⁸ finds that the ambient pressure, room-temperature Ce valence is 3.1, indicating that valence fluctuations are relatively weak. For this reason, the gap in $\text{Ce}_3\text{Bi}_4\text{Pt}_3$ is thought to be a primarily magnetic energy scale, roughly equivalent to the Ce ion Kondo temperature.

The high-pressure resistivity measurements presented here address two related points. First, for what range of gap magnitudes can the gap be associated with the Kondo temperature? Second, the low-temperature transport indicates that the Fermi level lies in states in the gap. As we use pressure to continuously modify the electronic environment

of these gap states, how does the transport evolve? $\text{Ce}_3\text{Bi}_4\text{Pt}_3$ is ideal for such a study, as Bethe ansatz⁹ and $1/N$ expansion¹⁰ calculations on the Anderson impurity model have provided a rather complete picture of Ce ion energetics, valid from the Kondo to mixed valence regimes.

EXPERIMENTAL DETAILS AND RESULTS

Large single crystals of $\text{Ce}_3\text{Bi}_4\text{Pt}_3$ were grown from a Bi flux, using high-purity starting materials, including zone-refined Ce. The samples were mechanically and chemically thinned to a final thickness of 0.003 in. and mounted for resistivity measurements in a high-pressure Bridgman anvil cell. Experimental pressures were determined *in situ* using a superconducting Pb manometer.¹¹ We measured the electrical resistivity $\rho(T)$ of two crystals of $\text{Ce}_3\text{Bi}_4\text{Pt}_3$ from the same preparation batch for temperatures between 1.2 and 300 K and the results are shown in Figs. 1(a) and 1(b).

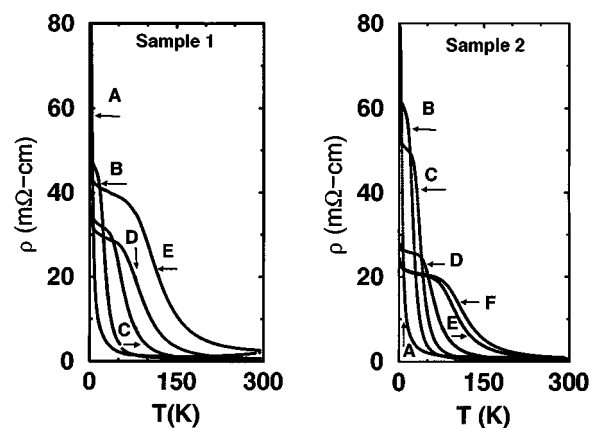


FIG. 1. Electrical resistivity of two single crystals of $\text{Ce}_3\text{Bi}_4\text{Pt}_3$. Applied pressures for sample 1 are A = 1 bar, B = 24 kbar, C = 37 kbar, D = 64 kbar, E = 117 kbar. Applied pressures for sample 2 are A = 3 kbar, B = 22 kbar, C = 36 kbar, D = 60 kbar, E = 117 kbar, and F = 145 kbar.

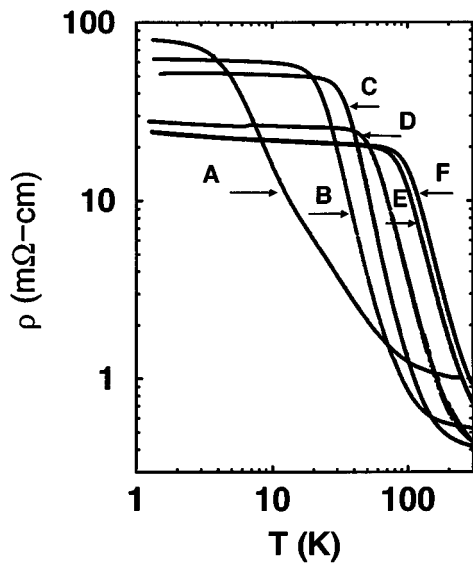


FIG. 2. Double logarithmic plot of $\rho(T)$ of sample 2. Applied pressures are $A=3$ kbar, $B=22$ kbar, $C=36$ kbar, $D=60$ kbar, $E=117$ kbar, and $F=145$ kbar.

Qualitatively, both samples show the previously reported behavior⁵ for ambient pressure $\text{Ce}_3\text{Bi}_4\text{Pt}_3$, namely, that $\rho(T)$ initially decreases as the temperature is reduced from room temperature, reaches a minimum value near 70 K, and monotonically increases with further reduction in temperature. With increased pressure, the overall strength of this temperature dependence is moderated and a low-temperature plateau in $\rho(T)$ is observed. In both samples, the low-temperature resistivity is rapidly suppressed with pressure, although the effect of pressure is minimal above ≈ 100 kbar in sample 1 and 120 kbar in sample 2. At each pressure $\rho(T)$ continues to increase as the temperature is reduced, signalling that $\text{Ce}_3\text{Bi}_4\text{Pt}_3$ is always insulating. In sample 2, we observed sharp drops in the resistivity at low temperature, suggestive of filamentary superconductivity. The pressure-dependent temperature at which we observed the resistivity drop agrees very closely to the complicated pressure-critical temperature phase diagram of superconducting Bi.¹² We conclude that Bi flux remains in this sample, perhaps at the grain boundaries, but amounting to no more than a few weight percent. No sign of excess Bi was observed in sample 1.

The electrical resistivity of sample 1 is presented in the double logarithmic plot of Fig. 2 to highlight the remarkable changes in the low-temperature transport observed under pressure. At each pressure, a characteristic temperature can be identified that marks the crossover from the high-temperature $\rho(T)$, which we will argue arises from excitations across the electronic gap, to the low-temperature resistivity, which is mediated by extrinsic gap states. We will analyze the electrical resistivity in these two regimes in turn.

We begin by examining the high-temperature regime, where the transport is dominated by excitations across the gap. To establish this, we have plotted the temperature-dependent resistivity $\rho(T)$ in an activation plot, Fig. 3. At high pressures, an extensive linear regime is found, and an activation gap Δ can be readily identified, increasing with increasing pressure. At low pressures, the analysis is more complicated, as the range of temperatures sandwiched be-

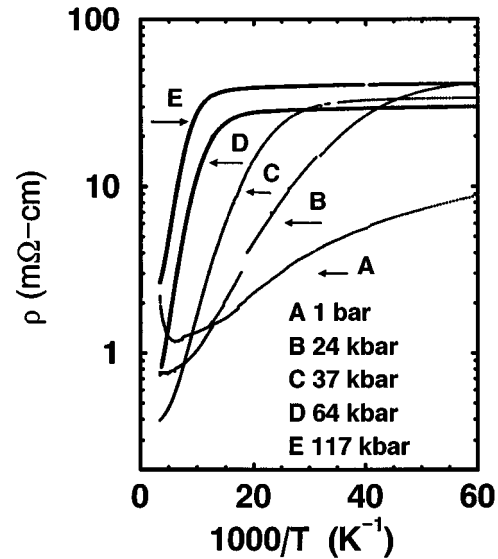


FIG. 3. Activation plot of $\rho(T)$ of sample 1. Applied pressures are $A=1$ bar, $B=24$ kbar, $C=37$ kbar, $D=64$ kbar, $E=117$ kbar.

tween the low-temperature transport regime and the condition for activated resistivity, that $T < \Delta$, becomes more limited. Using resistivity and thermopower measurements analyzed using degenerate semiconductor statistics, Hundley *et al.* showed⁵ that at ambient pressure Δ increases with decreasing temperature and consequently that the ambient pressure resistivity is not simply activated, in agreement with theoretical predictions.³ Above approximately 30 kbar, the analysis is simpler, as a clear range of temperatures can be identified in Fig. 3 for which activated resistivity is observed. We report the pressure dependence of the corresponding temperature-independent gap in Fig. 4, for two different crystals of $\text{Ce}_3\text{Bi}_4\text{Pt}_3$. For both samples, the gap is found to increase dramatically with pressure. In sample 2, 145 kbar is sufficient pressure to raise the gap from its ambient pressure value of 50 K more than a full order of magnitude to 560 K. The gap in sample 1 is no less pressure dependent, but the overall scale for the gap is somewhat reduced, relative to sample 2. We note that our measurements of the pressure

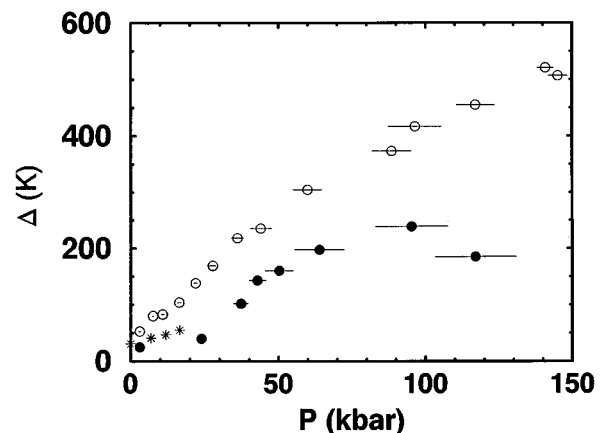


FIG. 4. Pressure dependence of the activation gap Δ for sample 1 (filled circles) and sample 2 (open circles). The asterisks represent $\Delta(P)$ from Ref. 13.

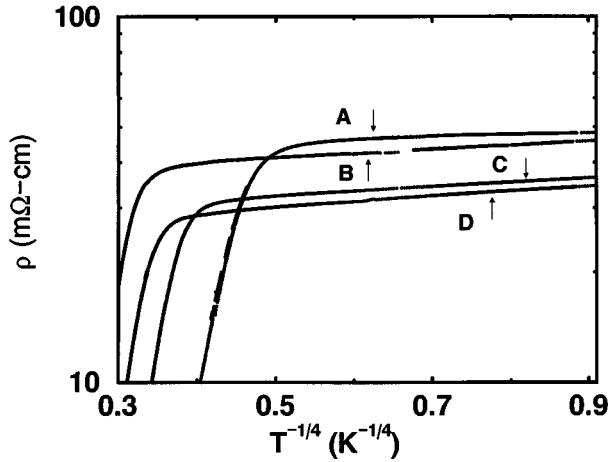


FIG. 5. Demonstration of a variable range-hopping contribution to $\rho(T)$ in sample 1 at low temperatures and high pressures. $A = 43$ kbar, $B = 50$ kbar, $C = 64$ kbar, $D = 117$ kbar.

dependence of Δ are in qualitative agreement with a previous resistivity study at pressures below 15 kbar,¹³ whose results are reproduced in Fig. 4. A comparison of the three samples represented in Fig. 4 suggests that there is considerable sample dependence not only in the magnitude of the activation gap, but also in its pressure dependence. A possible explanation is that impurities or defects provide a positive chemical pressure in samples like sample 1, and that this chemical pressure adds to the applied pressure in its effect on the electronic structure.

Turning now to the low-temperature transport, we have plotted the logarithm of the electrical resistivity as a function of $T^{1/4}$ in Fig. 5 to demonstrate that the transport in this temperature range is by three-dimensional variable range hopping, which is characterized by $\rho(T) = \rho_0 \exp[(T_0/T)^{1/4}]$. As is clear from Fig. 5, it is not possible to make this claim below ≈ 30 kbar in either sample over a meaningfully large range of temperatures. However, at 145 kbar, variable range hopping dominates the transport in sample 2 between 40 and 1 K. Attempts to describe the data using power laws, or modifications of variable range hopping including interactions or limited dimensionality were uniformly less successful than the analysis presented here.

THE ORIGIN OF Δ AND ITS PRESSURE DEPENDENCE

The electronic structure of Kondo insulators, of which $\text{Ce}_3\text{Bi}_4\text{Pt}_3$ at ambient pressure is taken to be the archetype, arises from the hybridization of a regular lattice of f -electron moments coupled to the conduction electrons.²⁻⁴ If there is one conduction electron per f -moment, the hybridized band structure is half-filled and the material, like $\text{Ce}_3\text{Bi}_4\text{Pt}_3$, is insulating. The gap Δ reflects the energetics of individual, compensated f -moments, and in the limit of weak hybridization is approximated by the Kondo temperature T_K . However, a more general expression for Δ , the fundamental energy scale for Ce moments, has been obtained from $1/N$ expansions, valid for arbitrarily strong charge and spin fluctuations,¹⁰

$$\epsilon_f - \Delta = -Nn(E_F)V^2 \ln[(D + \Delta)/\Delta]. \quad (1)$$

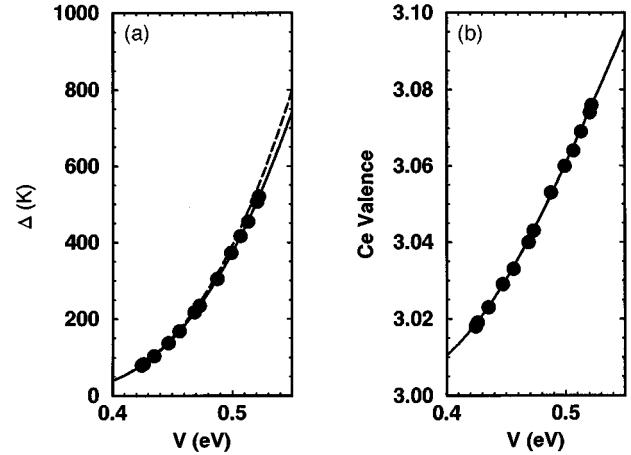


FIG. 6. (a) A comparison of the Kondo temperature T_K (dashed line) and the gap Δ (solid line) for the Ce impurity Anderson model as a function of the $4f$ -electron/conduction-electron hybridization. Filled circles are values of the gap Δ measured for sample 2 as a function of pressure. (b) The estimated increase in the Ce valence in $\text{Ce}_3\text{Bi}_4\text{Pt}_3$ for the pressure-dependent hybridization deduced from the measured $\Delta(P)$.

The parameters in this expression are those of the Anderson impurity model. By analyzing the specific heat, magnetic susceptibility, and transport properties of $\text{Ce}_3\text{Bi}_4\text{Pt}_3$, Sanchez-Castro, Bedell, and Cooper¹⁴ deduced ambient pressure values of the model parameters of the conduction electron density of states $N(E_F) = 1.02/\text{eV}$ and $D = 2\text{ eV}$. Although this analysis suggests that the f -electron energy ϵ_f is 0.2 eV below the chemical potential, photoemission measurements on similar $\text{Ce}_3\text{Bi}_4\text{Pt}_3$ samples¹⁵ indicate that $\epsilon_f = 2.08\text{ eV}$, similar to values found in a wide variety of Ce intermetallics. We take the ground-state Ce ion degeneracy N to be 2. If we make the well-established assumption for Ce compounds that the primary effect of pressure is to increase the hybridization V , while leaving the other parameters essentially unaffected,¹⁶ then we can use our measurements of the pressure dependence of Δ to determine the magnitude of the variation of V in our experiment. Note that the conduction-electron-local-moment hybridization $V = 0.425\text{ eV}$ required to reproduce the measured ambient pressure gap Δ is almost four times larger than that suggested by Sanchez-Castro, Bedell, and Cooper, $V = 0.112\text{ eV}$.

The Kondo temperature T_K and the gap Δ are plotted as functions of V in Fig 6. Values of the gap observed in our experiments on sample 2 are also plotted, indicating that there is approximately a 30% increase in hybridization over the pressure range studied in our experiment. Only at the largest values of V is it possible to discern a difference between $T_K(V)$ and $\Delta(V)$, suggesting that the role of charge fluctuations is minimal in determining the energetics of $\text{Ce}_3\text{Bi}_4\text{Pt}_3$, even at the highest pressures. Knowing the pressure dependence of V , we can deduce the pressure-induced change in the Ce valence by comparing the pressure dependences of the charge energy scale NV^2/D and the spin energy scale T_K . The deviation from integral f -site occupancy n_f satisfies¹⁷

$$n_f = N\rho_0 V^2 / (\Delta + N\rho_0 V^2). \quad (2)$$

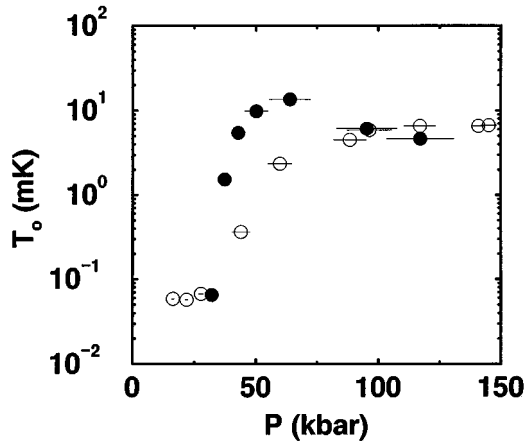


FIG. 7. The pressure dependence of the variable range-hopping parameter T_0 for sample 1 (filled circles) and sample 2 (open circles).

The computed Ce valence is plotted in Fig. 6 for the values of V implied by our measured $\Delta(P)$. The application of 145 kbar raises the Ce valence from its ambient pressure value of 3.01–3.08. Core-level spectroscopy measurements⁸ find the ambient pressure Ce valence to be 3.1. In lieu of detailed spectroscopic determination of the model parameters, it is not possible at this point to determine whether the difference between the calculated and measured Ce valence reflects any fundamental limitation to applying the Anderson impurity model to understanding the energetics of $\text{Ce}_3\text{Bi}_4\text{Pt}_3$. Our results indicate that the strong pressure dependence of the gap in $\text{Ce}_3\text{Bi}_4\text{Pt}_3$ is wholly consistent with the strong hybridization dependence of the Ce ion Kondo temperature, and for the pressure range studied here, the gap excitations affect primarily the conduction electron spin, but not the Ce ion valence.

LOW-TEMPERATURE TRANSPORT AND THE IN-GAP STATES

Our analysis of the pressure dependence of the gap in $\text{Ce}_3\text{Bi}_4\text{Pt}_3$ is consistent with the view that the gap increases due to increased hybridization between the f -electron and conduction-electron states. The effect that the modified electronic environment has on the transport properties of in-gap states is a sensitive probe of the nature and origin of those states. As depicted in Fig. 5, the low-temperature transport is dominated by the variable range-hopping mechanism, implying that transport involves direct overlap of the gap-state wave functions, not requiring excursions by the carriers into the conduction band. The characteristic length scale for the gap states, the localization length ξ_{loc} , can be found by noting that¹⁸

$$\rho(T) = \rho_0 \exp(T_0/T)^{1/4} \quad \text{with} \quad k_B T_0 = 1.5/N(E_F) \xi_{\text{loc}}^3. \quad (3)$$

The pressure dependence of T_0 is plotted in Fig. 7. T_0 is larger and more pressure dependent in sample 1. Despite the difference in magnitude of T_0 between the two samples, the characteristic length scale ξ_{loc} associated with the in-gap states has a maximum in both samples in our experimental

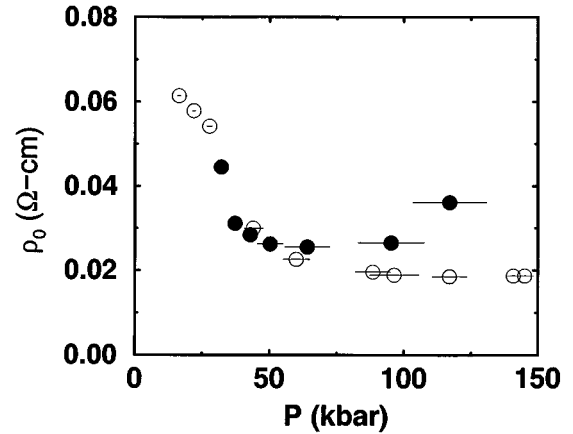


FIG. 8. The pressure dependence of the extrapolated zero-temperature resistivity ρ_0 for sample 1 (filled circles) and sample 2 (open circles).

pressure range. This trend is mirrored by the pressure dependence of the extrapolated zero-temperature resistivity ρ_0 , plotted in Fig. 8. For both samples, ρ_0 decreases with pressure, having very similar values below ~ 60 – 70 kbar. While ρ_0 approaches a constant, high-pressure value in sample 2, it increases in sample 1 at high pressure. It has been suggested¹⁹ that the extrapolated residual resistivity is a sensitive probe of sample quality in related compounds like SmB_6 . Figure 8 shows that this is not the case for $\text{Ce}_3\text{Bi}_4\text{Pt}_3$, in which the sample dependence of ρ_0 is relatively minor. Over the entire experimental pressure range, ρ_0 in both $\text{Ce}_3\text{Bi}_4\text{Pt}_3$ samples is orders of magnitude smaller than the maximum metallic resistivity, seemingly ruling out substantial many-body character for the gap states.²⁰

The pressure dependences of the variable range-hopping parameters T_0 and ρ_0 argue that the gap states are initially delocalized by pressure, but are ultimately localized at the highest pressures. We can understand this result in a very general way if the gap states derive a substantial part of their spatial extent from hybridization with conduction-electron states. While pressure can be expected to increase the spatial overlap of the local in-gap states and the itinerant conduction electrons, at the same time pressure quickly increases the energy separation of the two types of states, approximated by Δ . We suggest that at low pressures, the overlap between in-gap states, evidenced by the enhanced T_0 , is driven by their increased conduction-electron character, much as occurs in Si:P under uniaxial stress.²¹ This trend is reversed at high pressures, where the gap states act much as charged impurities in simple semiconductors. Here, enhancing the gap increases the dielectric constant and thus the spatial localization of the gap states. Since ξ_{loc} depends not only on the pressure-dependent spatial extent of the gap-state wave function but also on the pressure-independent concentration of the gap states we can formulate an explanation for the sample dependence apparent in Fig. 7. For a given value of the gap Δ , a sample with a lower concentration of gap states would be expected to have a smaller carrier localization length ξ_{loc} . For this reason, Fig. 9, which compares the pressure evolution of ξ_{loc} in our two samples suggests that

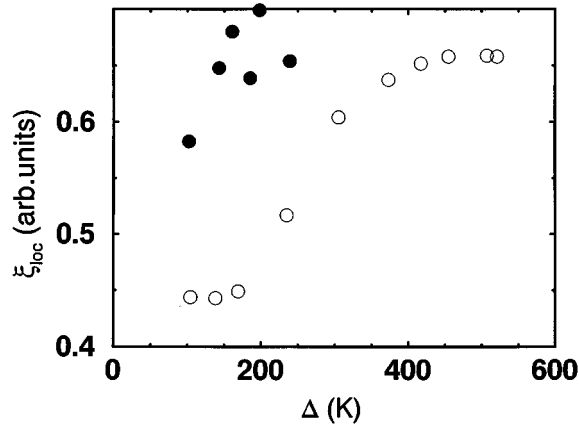


FIG. 9. The evolution of the electron localization length $\xi_0 \propto T_0^{1/3}$ as a function of activation gap Δ for sample 1 (filled circles) and sample 2 (open circles). The implicit variable is pressure, which varies between 1 bar and 117 kbar for sample 1, and 3 kbar and 145 kbar for sample 2.

sample 2 has a lower concentration of gap states, and presumably a lower concentration of defects and impurities, than sample 1.

Several proposals have been made regarding the origin of in-gap states in mixed valence and Kondo gap insulators. Recently, we have argued that the in-gap states in pressurized SmB_0 are precursors of the high-pressure, ungapped metal.²² We can rule this possibility out in $\text{Ce}_3\text{Bi}_4\text{Pt}_3$, as pressure increases the gap, ostensibly driving this system away from metallicity. Our high-pressure studies emphasize the importance of coupling between the in-gap and gap-edge states. If the defect has a magnetic moment, one approach²³ is to assume that the origin of the gap is independent of the coupling between the magnetic impurity and the conduction electron, which has its own scale, T_K . That is, the magnetic moment is partially compensated by a Kondo effect, which differs from that in a metal due to the presence of a gap in the conduction-electron density of states. All properties depend on Δ/T_K , which can either increase or decrease with pressure, depending on the exact symmetries of the magnetic moments and the rate at which pressure enhances Δ .

Another type of gap state, more specific to Kondo insulators, is the Kondo hole.²⁴ Here, the mixed conduction-

electron- f -electron character of the gap-edge states causes the formation of a localized state with magnetic character at the site of a nonmagnetic impurity. Doping studies provide evidence that $\text{Ce}_{3-x}\text{La}_x\text{Bi}_4\text{Pt}_3$ may host such Kondo hole states.⁵ While there is not a specific theoretical prediction for the effect of pressure on the transport properties of a Kondo hole, it is reasonable to expect that the spatial extent of the state should qualitatively follow that of the Kondo effect itself. Namely, pressure enhances long-range hybridization interactions, broadening and delocalizing the gap-edge states. However, at the same time, the pressure-induced increase of the gap seeks to localize all gap states, including the Kondo hole, and eventually is the dominant effect at sufficiently high pressure. Since the concentration of trace defect states is too low to determine their magnetic character, we have at present no means of distinguishing between these two possible descriptions of the in-gap states in $\text{Ce}_3\text{Bi}_4\text{Pt}_3$.

In summary, our measurements of the high-pressure resistivity of $\text{Ce}_3\text{Bi}_4\text{Pt}_3$ have revealed that there are two different transport mechanisms present, with gap excitations dominating the high-temperature transport and gap-state transport dominating the low-temperature transport. Pressure increases the electronic gap, and we find that the association of Δ with the Ce Kondo temperature is robust, even for a more than tenfold increase in the gap magnitude. Unlike other small gap systems in this family of materials, proximity to valence instability does not seem to be critical to the formation of the correlation gap in $\text{Ce}_3\text{Bi}_4\text{Pt}_3$. The low-temperature transport reveals the presence of extrinsic states in the gap. The spatial extent of the in-gap states arises from their coupling to extended, gap-edge states, a coupling that is strongly affected by pressure tuning of the gap. A more detailed examination of the magnetic properties of these in-gap states would be very useful for clarifying the extent to which their energetics are coupled to that of undoped $\text{Ce}_3\text{Bi}_4\text{Pt}_3$.

ACKNOWLEDGMENTS

We are grateful to Ward Beyermann for allowing us to reproduce his data in Fig. 4. M. C. A. thanks J. W. Allen, J. W. Rasul, P. Schlottmann, Z. Fisk, A. J. Arko, and P. Riseborough for helpful conversations. Work at the University of Michigan was supported by the U.S. Department of Energy, Office of Basic Energy Sciences, under Grant No. 94-ER-45526. Ames Laboratory is supported by the U.S. Department of Energy under Grant No. W-7405-Eng-82.

¹For a review of heavy fermions, see H. R. Ott and Z. Fisk, in *Handbook on the Physics and Chemistry of the Actinides*, edited by A. J. Freeman and G. H. Lander (North-Holland, Amsterdam, 1987), p. 85.

²G. Aeppli and Z. Fisk, *Comments Condens. Mater. Phys.* **16**, 155 (1992).

³P. Riseborough, *Phys. Rev. B* **45**, 13 984 (1992).

⁴A. J. Millis, in *Physical Phenomena at High Magnetic Fields*, edited by E. Manousakis *et al.* (Addison-Wesley, Redwood City, CA, 1992), p. 146.

⁵M. F. Hundley, P. C. Canfield, J. D. Thompson, Z. Fisk, and J. M. Lawrence, *Phys. Rev. B* **42**, 6842 (1990); M. F. Hundley, P. C. Canfield, J. D. Thompson, and Z. Fisk, *ibid.* **50**, 18 142 (1994).

⁶A. Severing, J. D. Thompson, P. C. Canfield, Z. Fisk, and P.

Riseborough, *Phys. Rev. B* **44**, 6832 (1991).

⁷B. Bucher, Z. Schlesinger, P. C. Canfield, and Z. Fisk, *Phys. Rev. Lett.* **72**, 522 (1994).

⁸G. H. Kwei, J. M. Lawrence, and P. C. Canfield, *Phys. Rev. B* **49**, 14 708 (1994).

⁹P. Schlottmann, *Phys. Rev. Lett.* **50**, 1697 (1983); *Z. Phys. B* **51**, 223 (1993).

¹⁰J. W. Rasul and A. C. Hewson, *J. Phys. C* **16**, L933 (1983); **17**, 2555 (1984); **17**, 3337 (1984).

¹¹T. F. Smith, C. W. Chu, and M. B. Maple, *Cryogenics* **9**, 53 (1969).

¹²N. Lotter and J. W. Wittig, *J. Phys. E* **22**, 440 (1989).

¹³W. P. Beyermann (private communication); J. D. Thompson, W. P. Beyermann, P. C. Canfield, Z. Fisk, M. F. Hundley, G. H.

- Kwei, R. S. Kwok, A. Lacerda, J. M. Lawrence, and A. Severing, in *Transport and Thermal Properties of f-Electron Systems*, edited by G. Oomi (Plenum, New York, 1993), p. 35.
- ¹⁴C. Sanchez-Castro, K. Bedell, and B. R. Cooper, *Phys. Rev. B* **47**, 6879 (1993).
- ¹⁵A. J. Arko (private communication).
- ¹⁶J. Röhler, in *Handbook on the Physics and Chemistry of the Rare Earths*, edited by K. A. Gschneidner, L. R. Eyring, and S. Hüffner (North-Holland, Amsterdam, 1987), Vol 10, p. 492.
- ¹⁷O. Gunnarsson and K. Schönhammer, *Phys. Rev. B* **28**, 4315 (1983).
- ¹⁸See, for instance, N. F. Mott, in *Metal-Insulator Transitions*, 2nd ed. (Taylor & Francis, London, 1990), p. 51.
- ¹⁹A. Kebede, M. C. Aronson, C. M. Buford, P. C. Canfield, J. H. Cho, B. R. Coles, J. C. Cooley, J. Y. Coulter, Z. Fisk, J. D. Goettee, W. L. Hults, A. Lacerda, T. D. McLendon, P. Tiwari, and J. L. Smith, *Physica B* **223-224**, 256 (1996).
- ²⁰C. M. Varma, in *Windsurfing the Fermi Sea*, edited by T. T. S. Kuo and J. Speth (North-Holland, Amsterdam, 1987), Vol. 1, p. 69.
- ²¹M. A. Paalanen, T. F. Rosenbaum, G. A. Thomas, and R. N. Bhatt, *Phys. Rev. Lett.* **48**, 1284 (1982); R. N. Bhatt, *Phys. Rev. B* **26**, 1082 (1982).
- ²²J. C. Cooley, M. C. Aronson, Z. Fisk, and P. C. Canfield, *Phys. Rev. Lett.* **74**, 1629 (1995).
- ²³K. Satori, H. Shiba, O. Sakai, and Y. Shimizu, *J. Phys. Soc. Jpn.* **61**, 3239 (1992); K. Takegahara, Y. Shimizu, N. Gto, and O. Sakai, *Physica B* **186-188**, 381 (1993).
- ²⁴See, P. Schlottmann, *J. Appl. Phys.* **75**, 7044 (1994), and references therein.